

Compression and Aggregation-Resistant Particles of Crumpled Soft Sheets

Jiayan Luo,^{†,∇} Hee Dong Jang,^{†,*,∇} Tao Sun,[‡] Li Xiao,[§] Zhen He,[§] Alexandros P. Katsoulidis,[⊥] Mercuri G. Kanatzidis,[⊥] J. Murray Gibson,^{‡,#} and Jiaying Huang^{†,*}

[†]Department of Materials Science and Engineering, Northwestern University, Evanston, Illinois 60208, United States, [‡]Advanced Photon Source, Argonne National Laboratory, Argonne, Illinois, 60439, United States, [§]Department of Civil Engineering and Mechanics, University of Wisconsin-Milwaukee, Milwaukee, Wisconsin, 53211, United States, [⊥]Department of Chemistry, Northwestern University, Evanston, Illinois 60208, United States, [¶]Department of Industrial Materials Research, Korea Institute of Geoscience and Mineral Resources, Yuseong-gu, Daejeon 305-350, Korea, and [#]College of Science, Northeastern University, Boston, Massachusetts 02115, United States. [∇]These authors contributed equally to this work.

A major problem in the scaled-up production of sheet-like materials, such as graphene, is their tendency to aggregate due to strong van der Waals attraction. Restacking of sheets not only reduces their solution processability, but also compromises their properties such as accessible surface area. Moreover, since materials typically experience some form of compressive stresses during manufacturing such as drying and pelletizing, their aggregation state tends to vary by processing history. Making layered materials aggregation-resistant will help to standardize the materials and their performance for large scale applications. A number of strategies for preventing aggregation in solution have been developed, which typically include reducing the size of the sheets, tailoring the solvent-graphene interactions, or employing dispersing agents.^{1–6} However, once the dispersions are dried, preventing aggregation of the solid state graphene product and making them redispersible are challenging. As is with the crumpled paper balls,^{7–9} the dimensional transition from flat sheets to three-dimensional (3D) crumpled particles, if achieved, could render them excellent compression and aggregation-resistant properties. Graphene oxide (GO) can be obtained in large quantities as colloidal dispersion in water, and is considered as a promising precursor for the bulk production of chemically modified graphene (*a.k.a.* reduced GO, r-GO).^{10–12} Crumpling of GO sheets in poor solvents was once proposed,¹³ but its success has remained uncertain.¹⁴ On the other hand, wrinkles and folds are commonly observed for GO and r-GO samples that have experienced some form of mechanical stress during solution

ABSTRACT Unlike flat sheets, crumpled paper balls have both high free volume and high compressive strength, and can tightly pack without significantly reducing the area of accessible surface. Such properties would be highly desirable for sheet-like materials such as graphene, since they tend to aggregate in solution and restack in the solid state, making their properties highly dependent on the material processing history. Here we report the synthesis of crumpled graphene balls by capillary compression in rapidly evaporating aerosol droplets. The crumpled particles are stabilized by locally folded, π – π stacked ridges as a result of plastic deformation, and do not unfold or collapse during common processing steps. In addition, they are remarkably aggregation-resistant in either solution or solid state, and remain largely intact and redispersible after chemical treatments, wet processing, annealing, and even pelletizing at high pressure. For example, upon compression at 55 MPa, the regular flat graphene sheets turn into nondispersible chunks with drastically reduced surface area by 84%, while the crumpled graphene particles can still maintain 45% of their original surface area and remain readily dispersible in common solvents. Therefore, crumpled particles could help to standardize graphene-based materials by delivering more stable properties such as high surface area and solution processability regardless of material processing history. This should greatly benefit applications using bulk quantities of graphene, such as in energy storage or conversion devices. As a proof of concept, we demonstrate that microbial fuel electrodes modified by the crumpled particles indeed outperform those modified with their flat counterparts.

KEYWORDS: graphene · graphene oxide · aerosol · capillary compression · crumpling · strain hardening · aggregation-resistant particles

processing,¹⁵ explosive thermal exfoliation,¹⁶ or compositing with polymer.¹⁷ In an earlier work, using fluorescence quenching microscopy (FQM), we directly observed that GO sheets in a drying droplet can be deformed by evaporation-induced capillary flow to generate a high wrinkled structure (also see Supporting Information, Figure S1).^{18,19} Therefore, if the evaporating droplets can be made free-standing, the soft GO sheets could be isotropically compressed to form a near-spherical particle just like a crumpled paper ball. This has now been achieved by an aerosol-assisted capillary compression process.

* Address correspondence to Jiaying-huang@northwestern.edu.

Received for review August 15, 2011 and accepted October 13, 2011.

Published online October 13, 2011
10.1021/nn203115u

© 2011 American Chemical Society

RESULTS AND DISCUSSION

Crumpled Particles from Rapidly Evaporating Aerosol Droplets. Figure 1a shows the experimental apparatus²⁰ and procedure. An aqueous dispersion of micrometer-sized GO sheets was nebulized to generate aerosol droplets and flown through a tube furnace preheated at 800 °C by N₂ carrying gas. Rapid evaporation causes shrinkage of the droplets, first concentrating the GO sheets and subsequently compressing them into crumpled balls of submicrometer scale. The GO sheets were also thermally reduced to chemically modified graphene (*a.k.a.* r-GO) as indicated by the color change from brown to black and confirmed by X-ray photoelectron spectroscopy. Indeed, scanning electron microscopy (SEM, Figure 1b) images of samples (1–4) captured along their flying pathway revealed their morphological evolution from (1) “coffee-ring”²¹ type of patterns, (2) clustered and tiled sheets, (3) aggregated and wrinkled sheets, to (4) the final three-dimensional, crumpled ball-like structure with many ridges and vertices. The morphological evolution suggests that each aerosol droplet produces one crumpled particle.

The size of the crumpled particles and the degree of crumpling can be tuned by the concentration of GO in the aerosol droplets as shown in Figure 2. With higher initial GO concentration, the average size of the crumpled particles became larger, and the degree of crumpling as indicated by the density of ridges and vertices was lower (Figure 2). The average size of the particles decreased from around 800 or 500 nm to 250 nm when the GO concentration was reduced from 5 or 1 mg/mL to 0.2 mg/mL, respectively. Since the GO sheets at least partially overlapped before crumpling (Figure 1b, 2 and 3), higher GO concentration would result in thicker GO flakes of higher bending modulus, making them stiffer against deformation, thus leading to the less crumpled, larger particles. In principle, it should be possible to produce crumpled particles made of only a single sheet at extremely low GO concentrations, which could show the highest degree of crumpling. Crumpled particles can be obtained with furnace temperature set as low as 100 °C, which is below the typical thermal reduction temperature of GO,^{22,23} suggesting that capillary compression rather than thermal annealing is responsible for deforming the sheets.

Microstructure Analysis on the Internal Structure of Crumpled Particles. The crumpled morphology is very open but also very robust as it can sustain common material processing conditions. SEM images in Figure 3 panels a, b, c, and d show that crumpled GO particles can survive solution processing, thermal shock,¹⁶ microwave heating,²⁴ and hydrazine vapor treatment,¹⁰ respectively, without unfolding or collapsing. In a paper ball, the crumpled structure is stabilized by plastically deformed ridges^{7–9} made of kinked paper fibers, which prevent the structure from unfolding. For crumpled

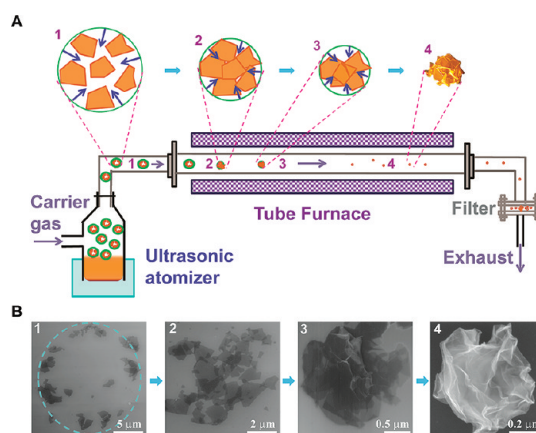


Figure 1. Particles of crumpled GO sheets by rapid isotropic compression in evaporating aerosol droplets. (a) Schematic drawings illustrating the experimental setup and the evaporation-induced crumpling process. Aerosol droplets containing GO sheets were nebulized and rapidly evaporated by passing through a preheated tube furnace. (b) SEM images of four samples collected along the flying pathway from spots 1 to 4 showing the typical morphologies of deposited GO evolving from (b1) sparse sheets in a “coffee-ring” pattern, (b2) clustered and tiled sheets, (b3) aggregated sheets with extensive wrinkles, to (b4) the final 3D crumpled, ball-like particle.

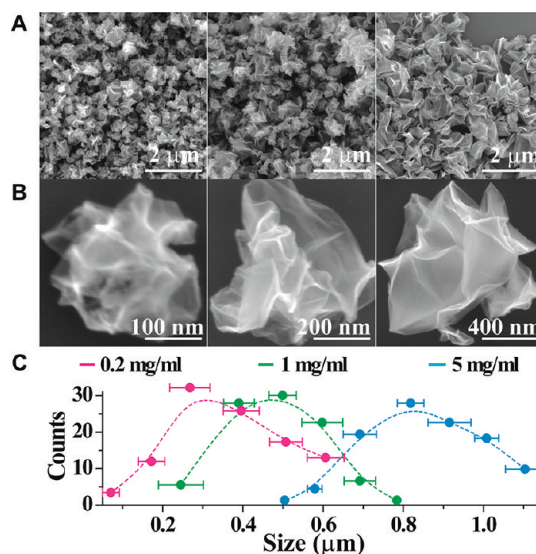


Figure 2. The size of the crumpled particles and the degree of crumpling can be tuned by the concentration of GO in the aerosol droplets as shown in the (a) low magnification overview and (b) representative high magnification single particle SEM images. (c) The average size of the particles decreased from around 800 or 500 nm to 250 nm when the GO concentration was reduced from 5 or 1 mg/mL to 0.2 mg/mL, respectively. The dotted lines are drawn as a guide to the eye.

graphene particles, the typical thicknesses of the ridges were found to be around tens of nanometers by electron microscopy. Since graphene can curve to form even smaller diameter carbon nanotubes without breaking chemical bonds,²⁵ the irreversible deformation in crumpled graphene balls should have a different mechanism. Scanning transmission electron microscopy

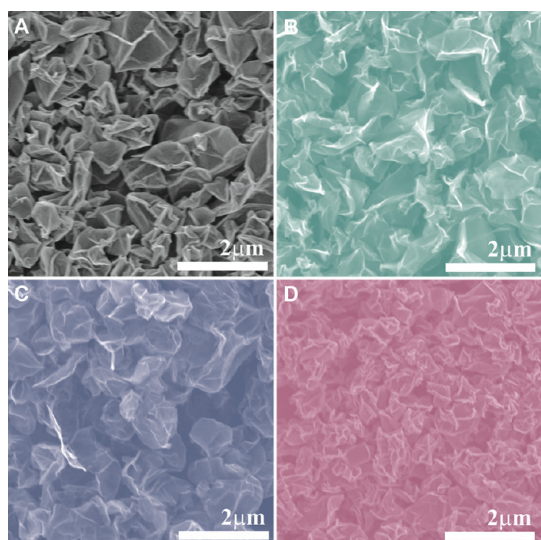


Figure 3. SEM images showing that crumpled morphology of GO is retained after (a) solution processing in methanol, (b) thermal shock at 400 °C, (c) microwave reduction, and (d) hydrazine reduction.

(STEM) and localized electron diffraction were performed to investigate the structure of ridges in crumpled r-GO. As shown in Figure 4a, a relatively flat particle was chosen over the more spherical crumples to avoid overlapping ridges in the projected STEM view. The convergent beam electron diffraction (CBED) patterns were then collected from a flat region (Figure 4c) and a ridge (Figure 4d), respectively. The pattern from the flat region contains a few sets of graphene (100) diffraction spots. The speckles at low- q regions are from amorphous carbon membrane used to support the sample. However, the pattern from the ridge shows strong graphite (002) diffraction spots corresponding to a d -spacing of around 3.5 Å, which is slightly larger than the standard 3.4 Å spacing in graphite crystal. This is attributed to less perfect stacking of r-GO sheets that still have residual surface functional groups.^{10–12} Next an electron diffraction contour map was constructed by scanning the electron beam across the entire area of the crumpled particle while collecting intensity from the (002) diffraction. Note that the electron atomic scattering factor had already been subtracted to remove the contribution of thickness/mass from the (002) scattering intensity. Therefore, the contour image directly maps out the distribution of tightly packed graphite-like domains in the crumpled particle. When this contour map is overlaid with the high-angle dark-field STEM image of the particle (Figure 4b), it clearly shows that all the spots giving high (002) scattering intensity are located along the ridges. This suggests that plastic deformation in the crumpled graphene particles is due to strong π - π stacking at the ridges.

Strain-Hardening Behavior of Crumpled GO Balls. A striking feature of crumpled paper balls is their increased stiffness and strength upon compression by forming more hard-to-bend ridges.^{7–9} This strain-hardening

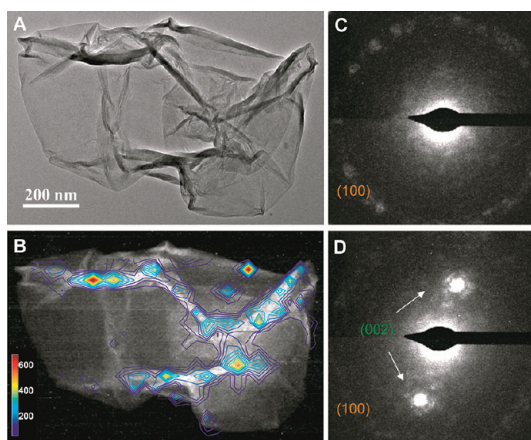


Figure 4. (a) TEM image of a particle of crumpled r-GO. Electron diffraction patterns from (c) a flat region and (d) a ridge on the crumple show that the graphene sheets are restacked at the ridges, yielding strong graphite (002) diffraction. This is further illustrated in (b) the high-angle dark-field image overlapped with the contour map of graphite (002) scattering intensity.

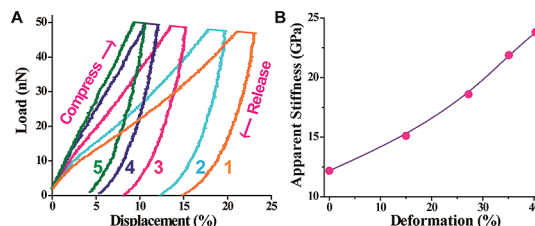


Figure 5. (a) Representative load/displacement curves of five cycles of compression and release on a single crumpled GO particle with a nanoindenter, showing that the particle was plastically deformed and strain hardened. (b) The apparent stiffness, calculated by dividing the slope of the initial linear segment of the loading curves by the initial cross-sectional area of the particle, also increased after each step of plastic deformation.

effect is also observed for crumpled GO balls in nanoindentation experiments. Figure 5a shows the load/displacement curves of a single crumpled GO particle compressed by a diamond nanoindenter. Five loading/hold/unloading cycles were performed with the maximal load of 50 nN. The displacement measures percent height reduction of the particle. In each cycle, a large plastic deformation was observed after an initial linear elastic response. As the cycling progressed, the degree of plastic deformation decreased continuously from 15% to less than 5%. Meanwhile, the apparent yield strength, marked by the load at the elastic-plastic transition on the loading curves increased after each cycle. Figure 5b shows that the apparent stiffness of the particle, calculated by dividing the slope of the initial linear segment of the loading curves within 2% displacement by the initial cross-sectional area of the particle, also increased after each cycle. Overall, the nanoindentation experiments revealed that the crumpled GO particles are compression-resistant just like paper balls⁸ as compressive stress makes them stiffer and harder.

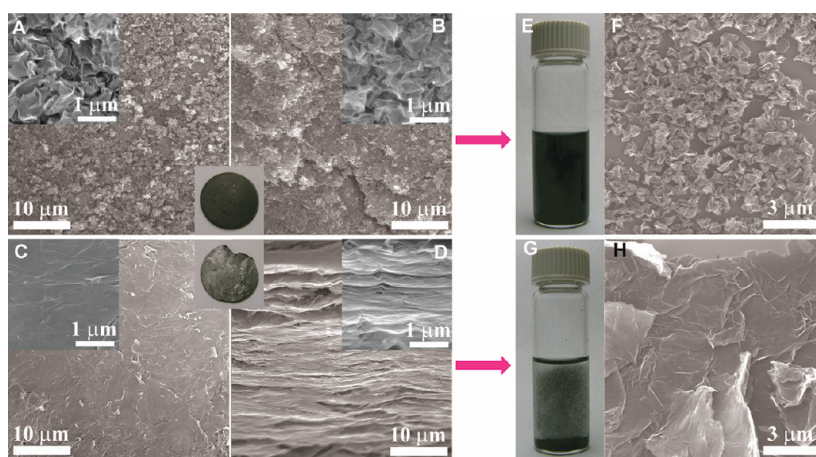


Figure 6. Compressed pellet of crumpled r-GO particles (inset of panels a and b) has rough and isotropic microstructures as shown in the SEM images taken at both (a) the surface and (b) cross section due to their near-spherical, pointy shape. In contrast, flat r-GO sheets restack along the compressing direction, resulting in a highly anisotropic pellet (inset of c, d) with (c) very smooth surface and (d) lamellar cross section. (e,f) The pellet of the crumpled particles can be readily dispersed by gentle hand-shaking after being compressed at 55 MPa. (g,h) However, the pellet of regular r-GO sheets cannot be redispersed due to extensive aggregation.

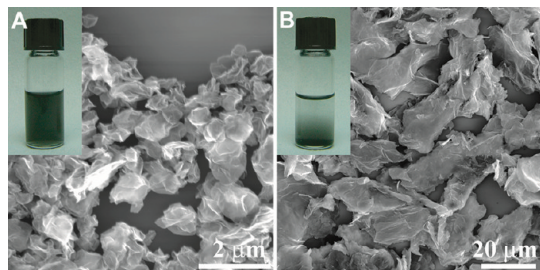


Figure 7. (a) SEM image shows that crumpled r-GO particles do not aggregate even after being compressed at 2 GPa. Therefore, they can be readily dispersed in solvents (see vial in inset) by gentle hand-shaking. (b) In contrast, sheet-like r-GO heavily aggregates, forming very large chunks that cannot be processed in solvents. Note that the scale bars of the two SEM images are different.

Compression and Aggregation-Resistant Particles of Crumpled Graphene Balls. The π - π stacked ridges and strain-hardening properties make the crumpled graphene balls remarkably stable against aggregation not only in solution but also in solid state. As shown in Figure 6a, b, when pelletized, crumpled graphene balls form a piece of isotropic, black solid with rough microstructures at both the surface and cross section. In contrast, sheet-like graphene yields an anisotropic, shiny pellet with very smooth, nearly featureless surface but laminated microstructure at the cross section (Figure 6c,d). Moreover, the pellet of crumpled balls, compressed at 55 MPa can be readily redispersed in solvents upon shaking by hand (Figure 6e). These include water, methanol, tetrahydrofuran, and even the poor solvents for GO or r-GO such as toluene, acetone, and cyclohexane. An SEM image of redispersed particles (Figure 6f) shows that the crumpled morphology is largely unaffected by the compression. In contrast, pellets of the r-GO sheets prepared under the same

pressure cannot be redispersed even after sonication due to extensive irreversible stacking (Figure 6g,h). To compare the effect of processing history on material properties, the redispersed samples as shown in Figures 6e and 6g were dried and pelletized again at 55 MPa. 4-Probe measurements showed that the surface conductivity of the pellet of crumpled particles was similar to that of a flat r-GO paper. The conductivity of recompressed r-GO sheets decreased by nearly 50%, which can be attributed to misaligned, aggregated graphene flakes after one cycle of dispersion/recompression. As expected, the conductivity of the crumpled r-GO pellet was largely unchanged. This suggests that crumpling a flat r-GO sheet can help to prevent aggregation without degrading the overall electrical conductivity. As shown in Figure 7, the crumpled particles can sustain compression at an even higher pressure of 2 GPa and still be readily redispersed in solution by just gentle shaking, while the regular graphene sheets became heavily aggregated and turned into large chunks of tens of micrometers in diameter.

The ease of aggregation of flat graphene-based sheets makes their properties, especially the surface area extremely sensitive to their processing history. The flowchart in Figure 8 shows the surface areas of regular and crumpled GO after various treatments. The starting regular GO sheets tightly stacked into a paper-like material, yielding a low specific surface area ($<5 \text{ m}^2/\text{g}$). If slowly heated, the resulting graphene product was poorly exfoliated and also had a very low surface area ($<5 \text{ m}^2/\text{g}$). To produce high surface area graphene, GO usually needs to be rapidly heated to trigger violent gas evolution for efficient exfoliation. After thermal shock, the surface area of the graphene product increased dramatically to $407 \text{ m}^2/\text{g}$, which however

was reduced by 44% to 226 m²/g after just one step of solution processing (*i.e.*, dispersing and drying) in methanol. Pelletizing the product at 55 MPa eliminated 84% of its original surface area, resulting in a low value of only 66 m²/g. In contrast, the crumpled GO balls already had a significantly higher starting surface area of 82 m²/g due to their open structure. They always yielded high surface area graphene products regardless of heating rate. Compared to the graphene sheets, crumpled balls had consistently higher and much more stable surface areas after the same processing steps.

Graphene Modified Microbial Fuel Cell (MFC) Electrodes. With their near-isotropic contour, remarkable aggregation-resistant behaviors and robust high surface area, properties of crumpled graphene balls have much less dependence on material processing history, therefore could help to standardize graphene-based materials, which will be critical for their large scale production.²⁶

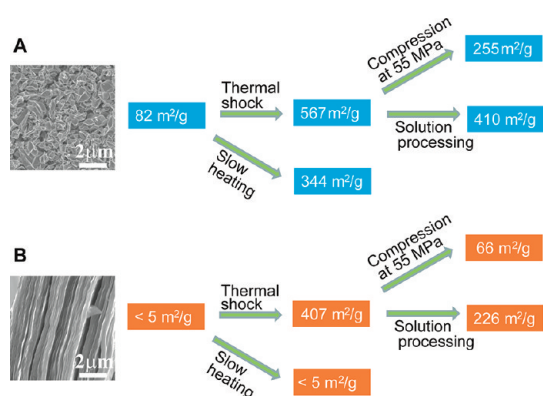


Figure 8. Evolution of the BET specific surface areas of (a) crumpled GO particles and (b) sheet-like GO after various material processing conditions including heating (at different rates), solution processing, and mechanical compression. After reduction, the crumpled particles maintained high surface area, regardless of the processing history. In contrast, the specific surface area of the sheet-like sample was highly dependent on processing history, and was lowered by 44% after only one step of solution processing, and drastically reduced by 84% after one step of compression at 55 MPa. Note that for both GO samples, the surface-adsorbed water would result in lower BET surface areas than their graphene products.

They can undergo common powder processing techniques such as solvent dispersion, molding, pelleting, and blending with other materials without significantly deteriorating properties, therefore should be beneficial for many applications such as polymer composites,¹⁷ catalytic supports,²⁷ and electrodes^{28–30} for batteries, capacitors, or fuel cells. As a proof-of-concept, here we show that MFCs (Figure 9a) made with crumpled graphene-modified anodes indeed outperform those modified by graphene. Compared to the commonly used anode modifiers such as activated carbon, crumpled graphene particles can offer many advantages because they provide not only high electron conductivity and high accessible surface area in solution, but also allow rapid mass transfer of the fuels and ions due to their open structure. In addition, they pack into a solid with rough surface, which can facilitate microbial diffusion and colonization. Indeed, anode modified by the crumpled graphene particles delivered superior performances of electricity generation to those covered with activated carbon and regular sheet-like graphene, leading to significantly higher short-circuit current (Figure 9b) and maximum power density (Figure 9c).

CONCLUSIONS

Particles of crumpled GO and r-GO (*i.e.*, chemically modified graphene) sheets have been obtained by capillary compression in rapidly evaporating aerosol droplets of GO. The average size of the crumpled, near-spherical particles is in the submicrometer range and can be tuned by the concentration of the starting GO concentration. As is with a crumpled paper ball, the crumpled graphene is also stabilized by plastically deformed ridges, and thus does not unfold or collapse during various types of solution processing or chemical or heating treatments. An electron diffraction study revealed strong graphitic (002) diffraction at the folded ridges, suggesting that they are held together by π - π stacking. The crumpled particles exhibit strain-hardening behaviors, thus making them remarkably resistant to aggregation in both solution and dried states.

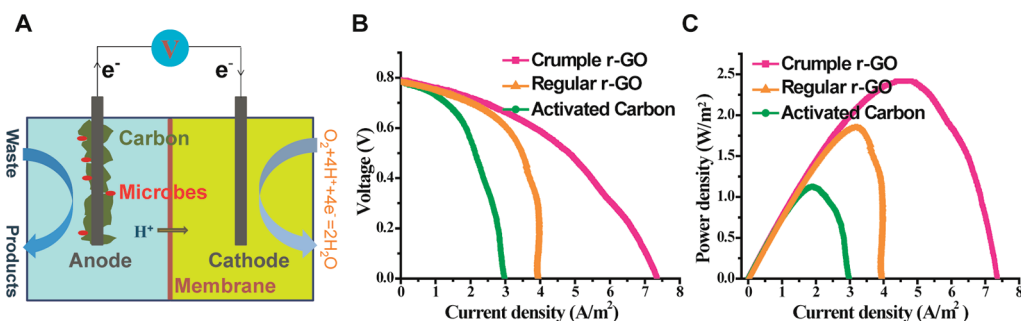


Figure 9. (a) Schematic diagram illustrating the structure of a MFC using an anode modified with crumpled graphene particles. (b) Compared to flat r-GO sheets or activated carbon, crumpled particles produce about twice of the short-circuit current. (c) Polarization curves show that the maximum power density of MFC made with crumpled r-GO anode is 31% and 116% higher than that prepared with regular r-GO and activated carbon, respectively.

They remain largely intact and redispersible after chemical treatments, wet processing, annealing, and even pelletizing at high pressure. Compared to the regular, flat sheets processed under the same conditions, the crumpled particles consistently have higher surface areas. In addition, the surface area of crumpled particles is more robust, and much less sensitive to the material processing history. The dimensional transition associated with the mechanical deformation effectively solves the aggregation problem of graphene without the need for any modification to material composition or surface properties. Therefore, such a

crumpled form of graphene should benefit applications relying on the high surface area of graphene. As a proof of concept, it is demonstrated that microbial fuel electrodes modified by the crumpled particles indeed outperform those modified with their flat counterparts.

Compared to common particulate materials, particles of crumpled sheets have an alternative set of rules governing their synthesis, structure, and properties. Therefore, they could also serve a model system to explore a new set of processing–structure-properties relationships of ultrafine particles.

METHODS

Synthesis of Crumpled Graphene Particles. GO was prepared by a modified Hummers' method³¹ as reported elsewhere.²² GO dispersions in water with various concentrations were nebulized by an ultrasonic atomizer (1.7 MHz, UN-511, Alfesa Pharm Co., Japan) to form aerosol droplets, which were carried by N₂ gas at 1 L/min to fly through a horizontal tube furnace (tube diameter = 1 in.) preheated at a desired temperature. The power of the nebulizer was set at the same level for all experiments. A Teflon filter was placed at the exhaust²⁰ to collect the crumpled particles.

Material Processing. Solution processing was typically done by first dispersing the powder samples in water or methanol by gentle shaking or sonication, and then filtration to collect the powders. The particles can also disperse in many other solvents known to be poor for dispersing GO or r-GO such as acetone, toluene, and cyclohexane. Slow heating was done in a N₂ atmosphere by first heating the GO samples from room temperature to 400 °C at a rate of 3 °C/min, and holding them at 400 °C for another 2 h. Thermal shock¹⁶ was done by rapidly inserting the samples into a hot tube furnace at 400 °C to trigger the explosive exfoliation, and heating them for another 5 min. Microwave reduction²⁴ of GO was done by irradiating the samples in a commercial microwave oven at 1250 W for 1 min. Hydrazine reduction² was done by fluxing GO in hydrazine at 80 °C for 12 h. Mechanical compression was done by pelletizing the dried samples in a die with a diameter of either 3 or 20 mm.

Characterization. SEM images were taken on a FEI NOVA 600 SEM microscope. The size distributions of crumpled particles were obtained by counting 100 particles of each sample in SEM images. To study the morphological evolution of GO, Si wafers were placed along the aerosol flying pathway as indicated by positions 1–4 in Figure 1, collecting samples before and during different stages of heating. A STEM study was conducted using a Tecnai F20ST microscope (FEI Company, USA) operated at an acceleration voltage of 200 kV. To generate the (002) contour map, 540 sets of CBED pattern were collected in STEM mode from an area of 1000 × 600 nm² with pitch of 33 nm. The probe size is about 4 nm, and the exposure time for each diffraction pattern is 5 s. The specific surface areas were measured using the Brumauer–Emmett–Teller (BET) method based on the nitrogen adsorption–desorption isotherms measured at 77 K on a Micromeritics TriStar II 3020 sorption analyzer. Nanoindentation experiments were conducted on a TI950 Triboindenter (Hysitron). A Berkovich diamond nanoindenter with an included angle of 142.35° and radius of 150 nm was used to locate and image the crumpled particles, and perform the indentation test.

MFC. A two-chamber MFC separated by a cation exchange membrane was constructed. Each chamber had a liquid volume of 120 mL. A commonly used carbon cloth anode (1.5 cm × 3 cm) was modified with activated carbon, regular r-GO, or crumpled r-GO, respectively, to improve its performance. A carbon brush was used as the cathode electrode. The MFC was operated in batch mode at room temperature. The anode was inoculated with the anaerobic sludge from a local

municipal wastewater treatment plant (South Shore Wastewater Treatment Plant, Milwaukee, WI, USA). The nutrient solution in the anode chamber contained sodium acetate as organic source and other mineral elements.³² The cathodic chamber was filled with potassium ferricyanide. All electrochemical tests were performed using a Gamry Reference 600 potentiostat.

Acknowledgment. This work was mainly supported by the new faculty startup fund (J.H.) from the Robert R. McCormick School of Engineering and Applied Science at Northwestern University and the General Project of the Korea Institute of Geoscience and Mineral Resources (KIGAM) (H.D.J.) funded by the Ministry of Knowledge Economy of Korea. Additional supports are provided from The Alfred P. Sloan Foundation, NSF (DMR CAREER 0955612) and The Sony Corporation (J.H.). J.L. thanks 3M for a graduate fellowship. Z.H. thanks the faculty start fund at the University of Wisconsin-Milwaukee. M.G.K. thanks DOE-EERE (Grant No. DE-FG36-08GO18137/A001) for support. The STEM study was accomplished at the Electron Microscopy Center for Materials Research at Argonne National Laboratory, a U.S. Department of Energy Office of Science Laboratory operated under Contract No. DE-AC02-06CH11357 by UChicago Argonne, LLC. We thank the NUANCE Center, which is supported by NSF-NSEC, NSF-MRSEC, Keck Foundation, the State of Illinois, and Northwestern University for use of their microscopy and materials analysis facilities.

Supporting Information Available: FQM images (Figure S1) showing GO sheet being crumpled by receding contact line during solvent evaporation. This material is available free of charge via the Internet at <http://pubs.acs.org>.

REFERENCES AND NOTES

- Li, D.; Muller, M. B.; Gilje, S.; Kaner, R. B.; Wallace, G. G. Processable Aqueous Dispersions of Graphene Nanosheets. *Nat. Nanotechnol.* **2008**, *3*, 101–105.
- Tung, V. C.; Allen, M. J.; Yang, Y.; Kaner, R. B. High-Throughput Solution Processing of Large-Scale Graphene. *Nat. Nanotechnol.* **2009**, *4*, 25–29.
- Luo, J. Y.; Cote, L. J.; Tung, V. C.; Tan, A. T. L.; Goins, P. E.; Wu, J. S.; Huang, J. X. Graphene Oxide Nanocolloids. *J. Am. Chem. Soc.* **2010**, *132*, 17667–17669.
- Hamilton, C. E.; Lomeda, J. R.; Sun, Z. Z.; Tour, J. M.; Barron, A. R. High-Yield Organic Dispersions of Unfunctionalized Graphene. *Nano Lett.* **2009**, *9*, 3460–3462.
- Yang, X.; Zhu, J.; Qiu, L.; Li, D. Bioinspired Effective Prevention of Restacking in Multilayered Graphene Films: Towards the Next Generation of High-Performance Supercapacitors. *Adv. Mater.* **2011**, *23*, 2833–2838.
- Aksay, I. A.; Korkut, S.; Roy-Mayhew, J. D.; Dabbs, D. M.; Milius, D. L. High Surface Area Tapes Produced with Functionalized Graphene. *ACS Nano* **2011**, *5*, 5214–5222.

7. Tallinen, T.; Astrom, J. A.; Timonen, J. The Effect of Plasticity in Crumpling of Thin Sheets. *Nat. Mater.* **2009**, *8*, 25–29.
8. Matan, K.; Williams, R. B.; Witten, T. A.; Nagel, S. R. Crumpling a Thin Sheet. *Phys. Rev. Lett.* **2002**, *88*, 076101.
9. Lobkovsky, A.; Gentges, S.; Li, H.; Morse, D.; Witten, T. A. Scaling Properties of Stretching Ridges in a Crumpled Elastic Sheet. *Science* **1995**, *270*, 1482–1485.
10. Park, S.; Ruoff, R. S. Chemical Methods for the Production of Graphenes. *Nat. Nanotechnol.* **2009**, *4*, 217–224.
11. Li, D.; Kaner, R. B. Graphene-Based Materials. *Science* **2008**, *320*, 1170–1171.
12. Compton, O. C.; Nguyen, S. T. Graphene Oxide, Highly Reduced Graphene Oxide, and Graphene: Versatile Building Blocks for Carbon-Based Materials. *Small* **2010**, *6*, 711–723.
13. Wen, X.; Garland, C. W.; Hwa, T.; Kardar, M.; Kokufuta, E.; Li, Y.; Orkisz, M.; Tanaka, T. Crumpled and Collapsed Conformations in Graphite Oxide Membranes. *Nature* **1992**, *355*, 426–428.
14. Spector, M. S.; Naranjo, E.; Chiruvolu, S.; Zasadzinski, J. A. Conformations of a Tethered Membrane—Crumpling in Graphitic Oxide?. *Phys. Rev. Lett.* **1994**, *73*, 2867–2870.
15. Cote, L. J.; Kim, J.; Zhang, Z.; Sun, C.; Huang, J. X. Tunable Assembly of Graphene Oxide Surfactant Sheets: Wrinkles, Overlaps and Impacts on Thin Film Properties. *Soft Matter* **2010**, *6*, 6096–6101.
16. Schniepp, H. C.; Li, J. L.; McAllister, M. J.; Sai, H.; Herrera-Alonso, M.; Adamson, D. H.; Prud'homme, R. K.; Car, R.; Saville, D. A.; Aksay, I. A. Functionalized Single Graphene Sheets Derived from Splitting Graphite Oxide. *J. Phys. Chem. B* **2006**, *110*, 8535–8539.
17. Stankovich, S.; Dikin, D. A.; Dommett, G. H. B.; Kohlhaas, K. M.; Zimney, E. J.; Stach, E. A.; Piner, R. D.; Nguyen, S. T.; Ruoff, R. S. Graphene-Based Composite Materials. *Nature* **2006**, *442*, 282–286.
18. Kim, J.; Kim, F.; Huang, J. Seeing Graphene-Based Sheets. *Mater. Today* **2010**, *13*, 28–38.
19. Kim, J.; Cote, L. J.; Kim, F.; Huang, J. Visualizing Graphene Based Sheets by Fluorescence Quenching Microscopy. *J. Am. Chem. Soc.* **2010**, *132*, 260–267.
20. Jang, H. D.; Chang, H.; Cho, K.; Kim, F.; Sohn, K.; Huang, J. X. Co-Assembly of Nanoparticles in Evaporating Aerosol Droplets: Preparation of Nanoporous Pt/TiO₂ Composite Particles. *Aerosol Sci. Technol.* **2010**, *44*, 1140–1145.
21. Deegan, R. D.; Bakajin, O.; Dupont, T. F.; Huber, G.; Nagel, S. R.; Witten, T. A. Capillary Flow as the Cause of Ring Stains from Dried Liquid Drops. *Nature* **1997**, *389*, 827–829.
22. Kim, F.; Luo, J.; Cruz-Silva, R.; Cote, L. C.; Sohn, K.; Huang, J. Self-Propagating Domino-like Reactions in Oxidized Graphite. *Adv. Funct. Mater.* **2010**, *20*, 2867–2873.
23. Jung, I.; Field, D. A.; Clark, N. J.; Zhu, Y. W.; Yang, D. X.; Piner, R. D.; Stankovich, S.; Dikin, D. A.; Geisler, H.; Ventrone, C. A.; Ruoff, R. S. Reduction Kinetics of Graphene Oxide Determined by Electrical Transport Measurements and Temperature Programmed Desorption. *J. Phys. Chem. C* **2009**, *113*, 18480–18486.
24. Zhu, Y. W.; Murali, S.; Stoller, M. D.; Velamakanni, A.; Piner, R. D.; Ruoff, R. S. Microwave Assisted Exfoliation and Reduction of Graphite Oxide for Ultracapacitors. *Carbon* **2010**, *48*, 2118–2122.
25. Ajayan, P. M.; Iijima, S. Smallest Carbon Nanotube. *Nature* **1992**, *358*, 23–23.
26. Segal, M. Selling Graphene by the Ton. *Nat. Nanotechnol.* **2009**, *4*, 611–613.
27. Kou, R.; Shao, Y. Y.; Mei, D. H.; Nie, Z. M.; Wang, D. H.; Wang, C. M.; Viswanathan, V. V.; Park, S.; Aksay, I. A.; Lin, Y. H.; Wang, Y.; Liu, J. Stabilization of Electrocatalytic Metal Nanoparticles at Metal–Metal Oxide–Graphene Triple Junction Points. *J. Am. Chem. Soc.* **2011**, *133*, 2541–2547.
28. Stoller, M. D.; Park, S. J.; Zhu, Y. W.; An, J. H.; Ruoff, R. S. Graphene-Based Ultracapacitors. *Nano Lett.* **2008**, *8*, 3498–3502.
29. Vivekchand, S. R. C.; Rout, C. S.; Subrahmanyam, K. S.; Govindaraj, A.; Rao, C. N. R. Graphene-Based Electrochemical Supercapacitors. *J. Chem. Sci.* **2008**, *120*, 9–13.
30. Liu, C. G.; Yu, Z. N.; Neff, D.; Zhamu, A.; Jang, B. Z. Graphene-Based Supercapacitor with an Ultrahigh Energy Density. *Nano Lett.* **2010**, *10*, 4863–4868.
31. Hummers, W. S.; Offeman, R. E. Preparation of Graphitic Oxide. *J. Am. Chem. Soc.* **1958**, *80*, 1339–1339.
32. Zhang, F.; Jacobson, K. S.; Torres, P.; He, Z. Effects of Anolyte Recirculation Rates and Catholytes on Electricity Generation in a Litre-Scale Upflow Microbial Fuel Cell. *Energy Environ. Sci.* **2010**, *3*, 1347–1352.